

Vertex corrections in localized and extended systems

Andrew J. Morris,^{1,*} Martin Stankovski,¹ Kris T. Delaney,^{2,†} Patrick Rinke,³ P. García-González,⁴ and R. W. Godby¹¹Department of Physics, University of York, Heslington, York YO10 5DD, United Kingdom²Department of Physics, University of Illinois at Urbana-Champaign, Urbana, Illinois 61801, USA³Fritz-Haber-Institut der Max-Planck-Gesellschaft, Faradayweg 4-6, Dahlem, D-14195 Berlin, Germany⁴Departamento de Física Fundamental, UNED, Apartado 60141, E-28080 Madrid, Spain

(Received 25 January 2007; revised manuscript received 5 July 2007; published 8 October 2007)

Within many-body perturbation theory, we apply vertex corrections to various closed-shell atoms and to jellium, using a local approximation for the vertex consistent with starting the many-body perturbation theory from a Kohn-Sham Green's function constructed from density-functional theory in the local-density approximation. The vertex appears in two places—in the screened Coulomb interaction W and in the self-energy Σ —and we obtain a systematic discrimination of these two effects by turning the vertex in Σ on and off. We also make comparisons to standard GW results within the usual random-phase approximation, which omits the vertex from both. When a vertex is included for closed-shell atoms, both ground-state and excited-state properties demonstrate little improvement over standard GW . For jellium, we observe marked improvement in the quasiparticle bandwidth when the vertex is included only in W , whereas turning on the vertex in Σ leads to an unphysical quasiparticle dispersion and work function. A simple analysis suggests why implementation of the vertex only in W is a valid way to improve quasiparticle energy calculations, while the vertex in Σ is unphysical, and points the way to the development of improved vertices for *ab initio* electronic structure calculations.

DOI: [10.1103/PhysRevB.76.155106](https://doi.org/10.1103/PhysRevB.76.155106)

PACS number(s): 71.45.Gm, 31.25.Eb, 31.25.Jf, 71.10.Ca

I. INTRODUCTION

Many-body perturbation theory (MBPT) is a leading method for computing excited-state electronic properties in solid-state physics.¹⁻³ Within many-body perturbation theory, Hedin's GW method⁴ is the most widely used approximation for the self-energy Σ . The exact one-body Green's function G (which contains information about ground- and excited-state properties of the system) can be written, using a Dyson equation, in terms of a suitable Green's function of a "zeroth-order" system of noninteracting electrons, G_0 (constructed from that system's one-particle wave functions and energies), and the self-energy operator Σ . The approximation is defined by the choice of zeroth-order system and by the expression (typically a diagrammatic expansion in terms of G_0) used to approximate Σ . The self-energy Σ contains all the information of many-body interactions in the system and can be obtained by using Hedin's set of coupled equations,

$$\Sigma(12) = i \int W(1^+3)G(14)\Gamma(42;3)d(34), \quad (1)$$

$$W(12) = v(12) + \int W(13)P(34)v(42)d(34), \quad (2)$$

$$P(12) = -i \int G(23)G(42)\Gamma(34;1)d(34), \quad (3)$$

$$\Gamma(12;3) = \delta(12)\delta(13) + \int \frac{\delta\Sigma(12)}{\delta G(45)}G(46)G(75)\Gamma(67;3)d(4567), \quad (4)$$

and the Dyson equation, where P is the polarizability, W the

screened and v the unscreened Coulomb interactions, and Γ the vertex function. The notation $1 \equiv (\mathbf{x}_1, \sigma_1, t_1)$ is used to denote space, spin, and time variables and the integral sign stands for the summation or integration of all of these where appropriate (1^+ denotes $t_1 + \eta$, where η is a positive infinitesimal in the time argument). Atomic units are used in all equations throughout this paper. These are four coupled integrodifferential equations where the most complicated term is the *vertex* Γ , which contains a functional derivative and hence, in general, cannot be evaluated numerically. The vertex is the usual target of simplification for an approximate scheme.

The widely used GW approximation is derived with the Hartree method as a starting point and hence has a rigorous foundation only when started from a noninteracting Green's function, G_0 , made from eigenstates of the Hartree Hamiltonian. This is because the initial self-energy $\Sigma_0=0$ and the vertex function is correspondingly set to $\Gamma(12;3) = \delta(12)\delta(13)$ since $\delta\Sigma(12)/\delta G(45)=0$.

Solving Hedin's equations with the vertex fixed in this expression yields the so-called self-consistent GW approximation. In this approach, the self-energy operator is formed from a product of a Green's function and a screened Coulomb interaction, where the Green's function used is consistent with that returned by Dyson's equation. Since the self-energy depends on G , this procedure should be carried out self-consistently, beginning with $G=G_0$.

In practice, it is customary to use the first iteration only, often called $G_0W_0^{\text{RPA}}$, to approximate the self-energy operator. Here, W_0^{RPA} is perhaps the simplest possible screened interaction, which involves an infinite geometric series over noninteracting electron-hole pair excitations as in the usual definition of the random-phase approximation (RPA). It is important to make this one iteration as accurate as possible,

so an initial G_0 calculated using the Kohn-Sham density-functional theory in the local-density approximation (DFT-LDA) is normally used. This choice of G_0 generally produces much more accurate results for quasiparticle energies (the correct electron addition and removal energies, in contrast to the DFT-LDA eigenvalues⁵). However, because this choice of G_0 corresponds to a nonzero Σ_0 , there is no longer a theoretical justification for the usual practice of setting the vertex to a product of delta functions and different choices for the exchange-correlation functional may lead to different Green's functions.^{6,7}

Using the static exchange-correlation kernel K_{xc} (which is the functional derivative of the DFT exchange-correlation potential V_{xc} with respect to density n), Del Sole *et al.*⁸ demonstrated how $G_0W_0^{RPA}$ may be modified with a vertex function to make Σ consistent with the DFT-LDA starting point. They added the contribution of the vertex into both the self-energy Σ and the polarization P . The result is a self-energy of the form $G_0W_0\Gamma^{LDA}$.⁹ The $G_0W_0^{LDA}$ approximation is obtained when the vertex function is included in P only. As commented by Hybertsen and Louie¹⁰ and Del Sole *et al.*, both these results take the form of GW but with W representing the Coulomb interaction screened by, respectively, the test-charge-electron dielectric function and the test-charge-test-charge dielectric function, in each with electronic exchange and correlation included through the time-dependent adiabatic LDA (TDLDA).

Del Sole *et al.* found that $G_0W_0\Gamma^{LDA}$ yields final results almost equal to those of $G_0W_0^{RPA}$ for the band gap of crystalline silicon and that the equivalent results from $G_0W_0^{LDA}$ were worse when compared to $G_0W_0^{RPA}$. It should perhaps be mentioned that the inclusion of other types of vertex corrections has been studied before as well, most notably corrections based on various approximations of a second iteration of Hedin's equations, starting with $G_0W_0^{RPA}$.^{11,12} However, these have usually been applied with initial Kohn-Sham (KS) Green's functions, which are still not theoretically consistent with that starting point. The correct theoretical treatment of a second-iteration vertex from KS Green's functions is quite complicated and still absent in the literature.

The purpose of the present work is to make a systematic study, for both localized and extended systems, of a simple *ab initio* vertex correction whose form is determined by the starting approximation for the self-energy ($\Sigma_0 = V_{xc}$ for DFT-LDA). Related vertex corrections, including others derived from K_{xc} , have been investigated in an earlier work. For example, Northrup *et al.*¹³ used LDA bulk calculations as a starting point and a plasmon-pole calculation of the response function in conjunction with a $G_0W_0^{LDA}$ -like vertex correction in the screened interaction. They found a narrowing of the bandwidths of Na, Li, and K,¹⁴ in agreement with the experiments of Jensen and Plummer¹⁵ who had noted that the experimental bandwidth was significantly narrowed ($\sim 23\%$) compared to the free-electron result. Hedin's $G_0W_0^{RPA}$ (Ref. 4) calculations only gave a narrowing of about 10% for a homogeneous electron gas of the same mean density, indicating a large impact of further many-body effects. This led to additional experimental and theoretical investigations¹⁶⁻²¹ but the issue remains controversial.²²⁻²⁵

For individual atoms, GW quasiparticle properties have been investigated previously by Shirley and Martin²⁶ (in-

cluding an exchange-only vertex) and, more recently, total energy studies on atoms and molecules using the variational functionals of Luttinger and Ward²⁷ have been performed by Dahlen *et al.*,^{28,29} Stan *et al.*,³⁰ and Verdonck *et al.*³¹ These studies have shown that $G_0W_0^{RPA}$ in general gives quasiparticle properties which are much improved over DFT and Hartree-Fock methods and that, when calculated self-consistently, GW also provides reasonably good total energies (with differences versus highly accurate reference methods being on the order of tens of millihartree/electron). To its merit, self-consistent GW is also a conserving approximation in the Baym-Kadanoff³² sense. However, non-self-consistent total energies in $G_0W_0^{RPA}$ are noticeably less accurate. Conversely, the good agreement between the quasiparticle energies and experiment is destroyed when performing self-consistent calculations.

The answer to why this happens must, by definition, lie with the only approximated quantity, the vertex correction. This study is meant to address the need for a precise (including a full treatment in frequency) comparative study of the vertex corrections proposed by Del Sole *et al.* for localized and extended systems within G_0W_0 .

II. METHOD

Hybertsen and Louie¹⁰ comment that it is possible to start a GW calculation from an initial self-energy, $\Sigma_0(12) = \delta(12)V_{xc}(1)$. This approach gives a theoretical basis for beginning a G_0W_0 calculation from DFT-LDA orbitals. Adopting this idea, we see from Eq. (4) that the second term is now nonzero, unlike in the GW approximation. Since the electron density is $n(1) = -iG(11^+)$, then

$$\frac{\delta\Sigma(12)}{\delta G(45)} = \frac{\delta\Sigma(12)}{\delta n(4)} \frac{\delta n(4)}{\delta G(45)}, \quad (5)$$

$$= -i \frac{\delta V_{xc}^{LDA}(1)}{\delta n(4)} = -i K_{xc}^{LDA}(1), \quad (6)$$

where delta functions are to be understood in all other variables. In an appendix, Del Sole *et al.*⁸ show how to add this approximate vertex to both W and Σ , and into W only, by forming two different effective W 's. Our method follows that of Del Sole *et al.*⁸ by modifying the dielectric function ϵ from its form in the RPA. The screened Coulomb interaction in MBPT is written as

$$W = \epsilon^{-1}v, \quad (7)$$

where ϵ^{-1} is the inverse dielectric function. We use the full polarization without recourse to plasmon-pole models. The RPA dielectric function is

$$\epsilon = 1 - v\chi^0. \quad (8)$$

Del Sole *et al.* show that adding the form of the vertex from Eq. (6) into both Σ and W modifies the RPA dielectric function to

$$\tilde{\epsilon} = 1 - (v + K_{xc})\chi^0, \quad (9)$$

which leads to the introduction of an effective screened Coulomb interaction \tilde{W} . This is trivial to implement into a GW

computer code as it requires a simple matrix addition once K_{xc} is calculated. The result of this modification is that \tilde{W} contains not only the screened Coulomb interaction but also an exchange-correlation potential. We shall refer to this method as $G_0W_0\Gamma^{LDA}$ as we have added the correct DFT-LDA vertex to the GW method; hence, the method is a one-iteration GW ($G_0W_0\Gamma_0$) calculation beginning with a DFT-LDA Green's function.

An alternative choice for the effective dielectric function,

$$\tilde{\epsilon} = 1 - (1 - K_{xc}\chi^0)^{-1}v\chi^0, \quad (10)$$

corresponds to adding K_{xc} into W only. We term this method $G_0W_0^{LDA}$ as the LDA vertex is inserted into the screened Coulomb interaction W only. This is equivalent to the one-iteration GW approximation G_0W_0 but with W calculated using the adiabatic LDA.

The vertices presented are thus dynamical, i.e., frequency dependent, due to the inclusion of χ^0 , and must include the excitonic effects of the corresponding jellium due to the appearance of K_{xc} . Another way of looking at it is that this corresponds to a treatment beyond G_0W_0 where *at the level of the vertex corrections*, the system is modeled by the homogeneous electron gas. It is not likely, however, that these methods would be able to capture any satellite structure beyond that provided by K_{xc} as the calculations are non-self-consistent.

III. COMPUTATIONAL APPROACH

The quasiparticle energies ϵ_i and wave functions ψ_i are formally the solution of the quasiparticle equation,

$$\begin{aligned} & \left[-\frac{1}{2}\nabla^2 + V_{\text{ext}}(\mathbf{r}) + V_H(\mathbf{r}) \right] \psi_i(\mathbf{r}) + \int \Sigma(\mathbf{r}, \mathbf{r}'; \epsilon_i) \psi_i(\mathbf{r}') d\mathbf{r}' \\ & = \epsilon_i \psi_i(\mathbf{r}), \end{aligned} \quad (11)$$

where V_{ext} and V_H are the external and Hartree potentials, respectively.

In the case of a spherically symmetric system, it is sufficient to describe all nonlocal operators in the GW formalism by two radial coordinates and one angular coordinate, θ , that denotes the angle between the vectors \mathbf{r} and \mathbf{r}' . The self-energy Σ then assumes the much simpler form

$$\Sigma(r, r', \theta; \epsilon) = \sum_{l=0}^{\infty} [\Sigma_l(r, r'; \epsilon)] P_l(\cos \theta), \quad (12)$$

where $P_l(\cos \theta)$ is a Legendre polynomial of order l .

The Legendre expansion coefficients of the self-energy Σ are calculated directly, thereby circumventing the need for a numerical treatment of the angular dependence. We use a real-space and imaginary time representation³³ to calculate the self-energy from the noninteracting Green's function G_0 . The self-energy on the real-frequency axis, required for solving the quasiparticle equation, is obtained by means of analytic continuation.³³ The current implementation has been successfully applied to jellium clusters³⁴ and light atoms.^{7,35}

To obtain the quasiparticle energies and wave functions, the quasiparticle equation [Eq. (11)] is fully diagonalized in

the basis of the single particle orbitals of the noninteracting Kohn-Sham system. For localized systems, the quasiparticle wave functions can differ noticeably from the wave functions of the noninteracting system or in certain cases even have a completely different character, as was demonstrated for image states in small metal clusters.³⁴

Ground-state total energies were calculated using the Galitskii-Migdal formula³⁶ transformed to an integral equation over imaginary frequency. This avoids the analytic continuation of the self-energy, which would be unreliable for large frequencies.

For jellium, the homogeneous electron gas, we solve Heidin's equations in wave vector and real-frequency space. This avoids analytic continuation and enables accurate and easy extraction of spectral properties. Again, we do not use plasmon-pole models, but the full frequency-dependent polarization.

IV. TOTAL ENERGIES

The MBPT total energy results are compared against configuration interaction (CI) and quantum Monte Carlo (QMC) methods [variational Monte Carlo (VMC) and diffusion Monte Carlo (DMC)]. The CI and QMC families of methods usually yield the most accurate estimates of ground-state energies and are variationally bound, meaning that the lowest energy is the most accurate.

The G_0W_0 result with G_0 constructed from DFT-LDA eigenstates ($G_0W_0^{\text{RPA}}$) is in poor agreement with CI in all three cases. It is known that there is a large self-interaction error in the LDA, especially noticeable in smaller atoms. Hartree-Fock, which is self-interaction-free by construction, is more accurate than DFT-LDA. Hence, the self-interaction error is introduced via the LDA orbitals into the Green's function, G_0^{LDA} , which gives rise to the $G_0W_0^{\text{RPA}}$ total energy's consistent poor agreement with CI. [By way of illustration, using a G_0 from the superior Krieger, Li, and Iafrate (KLI) method,⁴³ an optimized effective potential that is formally free of self-interaction error for a two-electron system, greatly improves the DFT and GW total energies. The $G_0^{\text{KLI}}W_0^{\text{RPA}}$ results for He, Be, and Ne are $-1.4550(3)$, $-3.6780(2)$, and $-12.843(1)$, respectively.]

For all three atoms, the vertex in W alone ($G_0W_0^{\text{LDA}}$) shows little difference to $G_0W_0^{\text{RPA}}$ (Table I and Fig. 1), whereas $G_0W_0\Gamma^{\text{LDA}}$ raises the total energy with respect to $G_0W_0^{\text{RPA}}$. This change is due not to the LDA self-interaction but to the nature of the vertex. The result of adding the LDA vertex to $G_0^{\text{KLI}}W_0$ mirrors that of adding it to $G_0^{\text{LDA}}W_0$. There is an increase of the total energy when the vertex is applied in both W and Σ ($G_0^{\text{KLI}}W_0\Gamma^{\text{LDA}}$) but the vertex in W only ($G_0^{\text{KLI}}W_0^{\text{LDA}}$) results in a similar total energy to $G_0^{\text{KLI}}W_0^{\text{RPA}}$. [The total energies per electron for $G_0^{\text{KLI}}W_0\Gamma^{\text{LDA}}$ and $G_0^{\text{KLI}}W_0^{\text{LDA}}$ for He are $-1.4235(10)$ and $-1.4475(5)$, respectively.]

In jellium the trend is the same for all densities in the region from $r_s=2$ to 5 [r_s is the density parameter, where $r_s = (\frac{3}{4\pi n})^{1/3}$ and n is the electron density in a.u.], as can be seen in Table II. $G_0W_0^{\text{LDA}}$ lowers the total energy of jellium

TABLE I. Total energy data (hartrees/electron) (see Fig. 1—a comparison of various methods for total energy calculations). Hartree-Fock, density-functional theory, one-iteration GW ($G_0W_0^{\text{RPA}}$), the two approximate vertex GW methods, variational Monte Carlo, diffusion Monte Carlo, and configuration interaction. (CI usually yields the most accurate estimate of the ground-state energies for localized systems.)

Method	He	Be	Ne
HF	-1.4304 ^a	-3.6433 ^b	-12.8547 ^a
DFT-LDA	-1.4171	-3.6110	-12.8183
$G_0W_0^{\text{RPA}}$	-1.4117(5)	-3.5905(9)	-12.777(1)
$G_0W_0^{\text{LDA}}$	-1.4120(2)	-3.590(1)	-12.775(15)
$G_0W_0\Gamma^{\text{LDA}}$	-1.3912(2)	-3.573(1)	-12.745(10)
VMC	-1.45176 ^a	-3.66670 ^c	-12.891(5) ^a
DMC	-1.45186 ^a	-3.66682 ^c	-12.89231 ^a
CI	-1.45189 ^d	-3.66684 ^d	-12.89370 ^d

^aSee Ref. 37.

^bSee Ref. 38.

^cSee Ref. 39.

^dSee Ref. 40.

slightly as compared to $G_0W_0^{\text{RPA}}$ and $G_0W_0\Gamma^{\text{LDA}}$ makes the energy too high. $G_0W_0^{\text{RPA}}$ is on average $\sim 5\%$ lower than the QMC result. $G_0W_0\Gamma^{\text{LDA}}$ is $\sim 10\%$ too high and $G_0W_0^{\text{LDA}}$ is $\sim 6\%$ lower than the QMC result.

For jellium, neither method leads to a result more accurate than $G_0W_0^{\text{RPA}}$. It is apparent, however, that the vertex added solely in the polarization has the minor effect of lowering the

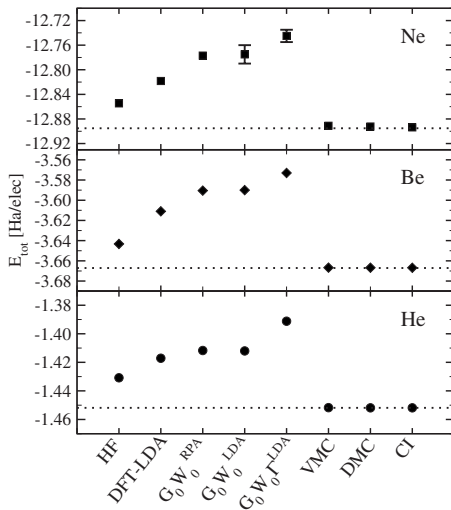


FIG. 1. Total energies of atoms. We compare a number of GW -based approaches to Hartree-Fock (Ref. 37), DFT with an LDA exchange-correlation functional consistent with the K_{xc} used, quantum Monte Carlo (Ref. 37) (VMC and DMC), and CI (Ref. 40). The dotted line is the CI value and is there to guide the eyes. In all cases, $G_0W_0\Gamma^{\text{LDA}}$ behaved poorly in comparison with $G_0W_0^{\text{RPA}}$, whereas $G_0W_0^{\text{LDA}}$ makes no improvement to $G_0W_0^{\text{RPA}}$. The MBPT methods are not as accurate as the computationally cheaper mean-field calculations but $G_0W_0^{\text{RPA}}$ and $G_0W_0\Gamma^{\text{LDA}}$ are the better of the three MBPT methods.

TABLE II. ϵ_{xc} (Ha), the exchange-correlation energy for jellium. The total energy per particle is given by $\epsilon = \frac{3}{5}\epsilon_F + \epsilon_{xc}$, where $\epsilon_F = \frac{1}{2}k_F^2 = \frac{1}{2}\left(\frac{1}{\alpha r_s}\right)^2$ and $\alpha = \left(\frac{4}{9\pi}\right)^{1/3}$. The energies under heading GW are from self-consistent calculations by García-González and Godby (Ref. 41) for reference. $G_0W_0^{\text{RPA}}$ is lower than the QMC energy by $\sim 5\%$ on average. $G_0W_0^{\text{LDA}}$ is $\sim 6\%$ lower and $G_0W_0\Gamma^{\text{LDA}}$ is $\sim 10\%$ too high. The DMC values are evaluated by Perdew and Zunger's (Ref. 42) parametrization of Ceperley and Alder's DMC calculations.

r_s	2	3	4	5
$G_0W_0^{\text{RPA}}$	-0.2826(3)	-0.1967(1)	-0.1522(1)	-0.1247(1)
$G_0W_0^{\text{LDA}}$	-0.2857(4)	-0.2002(2)	-0.1560(1)	-0.1288(1)
$G_0W_0\Gamma^{\text{LDA}}$	-0.2525(2)	-0.1678(1)	-0.1241(1)	-0.0972(1)
GW^a	-0.2727(5)	n/a	-0.1450(5)	-0.1185(5)
QMC (DMC) ^b	-0.2742(1)	-0.1902(1)	-0.1464(1)	-0.1202(1)

^aSee Ref. 41.

^bSee Ref. 42.

total energy. When the vertex is subsequently added into the self-energy there is a major positive shift in the total energy as seen in the atomic results as well. Self-consistent GW calculations^{41,44} for jellium show that the self-consistent total energy is about 4%–5% higher than the $G_0W_0^{\text{RPA}}$ ones in the range of $r_s=2-5$, and the essentially exact QMC energies are about 0.5%–1% lower than the self-consistent GW values. Assuming to a first approximation that the vertex corrections are independent and additive corrections to self-consistency, this would indicate that the $G_0W_0\Gamma^{\text{LDA}}$ energies would still be much too high, but the $G_0W_0^{\text{LDA}}$ energies might end up very close to the QMC results if self-consistency is achieved, since they lower the $G_0W_0^{\text{RPA}}$ energies to roughly the same extent as the difference between QMC and self-consistent GW energies.

V. QUASIPARTICLE ENERGIES

The quasiparticle energy corresponding to the first ionization energy⁶³ is presented for helium, beryllium, and neon in Fig. 2. The MBPT methods are consistently more accurate than DFT-LDA Kohn-Sham eigenvalues (Table III). However, again, $G_0W_0^{\text{LDA}}$ is roughly equivalent to $G_0W_0^{\text{RPA}}$ for helium and beryllium, and in all cases $G_0W_0\Gamma^{\text{LDA}}$ causes an increase in quasiparticle energy, in agreement with Del Sole *et al.*⁸ In general, $G_0W_0\Gamma^{\text{LDA}}$ worsens QP energies as compared to $G_0W_0^{\text{RPA}}$.

For jellium, different quantities are accessible at different stages of the iteration of Hedin's equations. The pair-correlation function $g(r)$, for example, can be obtained from the (isotropic) inverse dielectric function $\epsilon^{-1}(k, \omega)$ by the integration

$$g(r) = 1 + \frac{3}{2rk_F^3} \int_0^\infty dk k \sin(kr)[S(k) - 1], \quad (13)$$

where the static structure factor

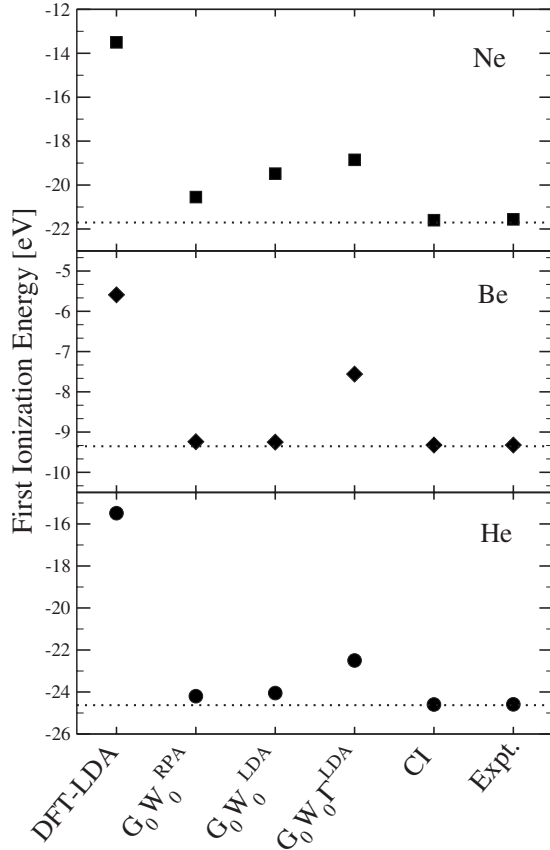


FIG. 2. QP energies of atoms. The first ionization energy is plotted. We compare the GW -based approaches to DFT-LDA; the experimental (Refs. 45–47) answer (Expt.) and the values calculated from the differences in CI (Ref. 40) calculations (CI). The helium, beryllium, and neon values are plotted with circles, diamonds, and squares, respectively. The dotted lines go through the CI value and are there to guide the eyes. All of the GW calculations are more accurate than the mean-field method. For helium and beryllium, the $G_0W_0^{RPA}$ and $G_0W_0^{LDA}$ methods give similar results. In all cases, $G_0W_0^{\Gamma LDA}$ is shifted to a higher energy than $G_0W_0^{RPA}$. [This shift for $G_0W_0^{\Gamma LDA}$ was also found by Del Sole *et al.* (Ref. 8) and Fleszar and Hanke (Ref. 49).]

$$S(k) = -\frac{k^2 r_s^3}{3} \int_0^\infty \frac{d\omega}{\pi} \Im[\varepsilon^{-1}(k, \omega)]. \quad (14)$$

$g(r)$ is shown in Fig. 3 for $r_s=1.0$. The RPA displays the well-known failure to be positive definite for $r_s \geq 0.78$. This is remedied by the local vertex, but the result appears to be an overcorrection (note that $G_0W_0^{LDA}$ and $G_0W_0^{\Gamma LDA}$ are equivalent at this stage since Σ has not yet been calculated).

The tendency of $G_0W_0^{\Gamma LDA}$ to overshoot—the reason for which we will defer to the closing discussions—is apparent in all subsequent results. Once Σ has been calculated, the QP dispersion can be extracted. Presented in Fig. 4 is the real part of the self-energy evaluated at the self-consistent eigenvalues, i.e., the correction $\text{Re}[\Sigma_{\mathbf{k}}(\varepsilon_{\mathbf{k}})]$ to the quasiparticle dispersion as found by

TABLE III. First ionization energy (eV), a comparison of various methods for quasiparticle energy calculations: DFT-LDA, $G_0W_0^{RPA}$, and the two approximate GW methods. CI denotes the ionization potential calculated from the difference in CI total energies and Expt. is the measured value.

Method	He	Be	Ne
DFT-LDA	-15.4877	-5.909	-13.503
$G_0W_0^{RPA}$	-24.20(4)	-9.24(2)	-20.55(10)
$G_0W_0^{LDA}$	-24.05(5)	-9.25(3)	-19.48(10)
$G_0W_0^{\Gamma LDA}$	-22.5(1)	-7.56(6)	-18.85(5)
CI	-24.5930 ^a	-9.3226 ^a	-21.6034 ^a
Expt.	-24.587 ^b	-9.3227 ^c	-21.5645 ^d

^aSee Ref. 40.

^bSee Refs. 45 and 46.

^cSee Ref. 47.

^dSee Ref. 48.

$$\varepsilon_{\mathbf{k}} = \varepsilon_{\mathbf{k}}^0 + \text{Re}[\Sigma_{\mathbf{k}}(\varepsilon_{\mathbf{k}})], \quad (15)$$

where $\varepsilon_{\mathbf{k}}^0$ is the noninteracting dispersion. Care has been taken to align the Fermi energy of noninteracting and interacting systems so that the Dyson equation is consistent³⁶ and all quantities are calculated in real frequency. The self-consistent quasiparticle energy should be used when one has a self-consistent Σ , but for a G_0W_0 calculation there is still controversy about whether the self-consistent eigenvalues $\varepsilon_{\mathbf{k}}$ or the zeroth-order eigenvalues $\varepsilon_{\mathbf{k}}^0$ are best used as the argument of $\Sigma_{\mathbf{k}}$ in Eq. (15).^{1,50} The self-consistent approach was chosen in this paper.

The difference between the quasiparticle energies at $k=k_F$ and $k=0$ is known as the bandwidth, which therefore takes the form of the free-electron value ($k_F^2/2$) corrected by the change in Fig. 4 between $k=k_F$ and $k=0$. This bandwidth is shown in Table IV and Fig. 5. It consistently seems that vertex corrections applied in the screened Coulomb interaction *only* give the best results. This is corroborated by the fact that this quasiparticle dispersion has a better bandwidth

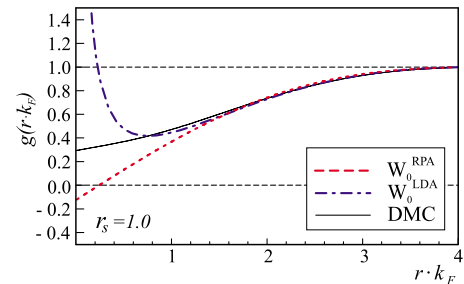


FIG. 3. (Color online) The pair-correlation function—evaluated at $r_s=1.0$. The RPA goes negative for small r , which is a well-known unphysical behavior of this approximation. Including the vertex makes the W_0^{LDA} fit the (essentially exact) QMC (Ref. 51) curve better, but then the p.-c. function goes too positive instead. The W_0^{LDA} curve does not go to infinity when $r \rightarrow 0$, it just goes to a very high value (~ 2000). The horizontal lines are there to guide the eyes.

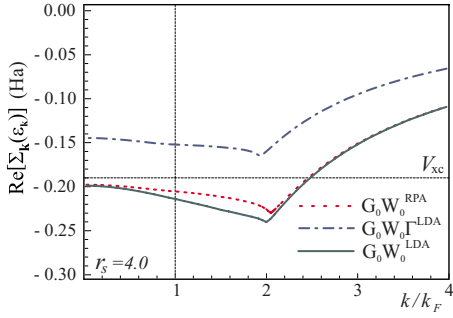


FIG. 4. (Color online) Correction to the free-electron quasiparticle dispersion for $r_s=4.0$ —note the large absolute shift for $G_0W_0\Gamma^{\text{LDA}}$. The two intersecting straight lines are included to emphasize that none of the dispersions fulfill the condition $\text{Re}[\Sigma_{\mathbf{k}_F}(\varepsilon_F)] = V_{\text{xc}}$.

and that the $G_0W_0\Gamma^{\text{LDA}}$ introduces little change to the bandwidth. These results are in agreement with those of Mahan and Sernelius⁵² obtained for a model Hubbard vertex.

VI. CHEMICAL POTENTIAL OF JELLIUM

To get another indication of whether the large absolute positive shift of the quasiparticle dispersion is physical, we compare with experimental work functions of Al (100), (110), and (111) surfaces (see Table V). We assume that the electron density of the surface region and therefore the electrostatic surface-dipole energy barrier are well described by LDA calculations including the crystal lattice. The work function ϕ will, however, be sensitive to the quasiparticle bulk Fermi level, which we use here as a discriminator between self-energy approximations in the bulk. Treating the bulk metal as jellium, we obtain a shift in the work function due to the new chemical potential,

$$\phi = \phi^{\text{LDA}} + \Delta\mu = \phi^{\text{LDA}} - \{\text{Re}[\Sigma_{\mathbf{k}_F}(\varepsilon_F)] - V_{\text{xc}}\}, \quad (16)$$

where $\Delta\mu$ is the correction due to the shift of the bulk Fermi energy for a GW jellium calculation. The LDA work function is defined as the shift between the vacuum potential ϕ_{vac} and

TABLE IV. Occupied bandwidths of jellium for different r_s (eV)—evaluated at the self-consistent eigenenergy.

r_s	$G_0W_0^{\text{RPA}}$	$G_0W_0\Gamma^{\text{LDA}}$	$G_0W_0^{\text{LDA}}$	Expt.
(Al) 2.07	11.5445	11.6444	11.1814	$10.60 \pm 0.10^{\text{a}}$
(Li) 3.28	4.4644	4.4853	4.2129	$3.00 \pm 0.20^{\text{b}}$
(Na) 3.96	2.9837	2.9889	2.7777	$2.65 \pm 0.05^{\text{c}}$
(K) 4.96	1.8625	1.8579	1.7044	$1.60 \pm 0.05^{\text{d}}$
(Rb) 5.23	1.6669	1.6610	1.5191	$1.70 \pm 0.20^{\text{e}}$
(Cs) 5.63	1.4287	1.4215	1.2944	$1.35 \pm 0.20^{\text{e}}$

^aSee Ref. 53.

^bSee Ref. 54.

^cSee Ref. 21.

^dSee Ref. 20.

^eSee Ref. 55.

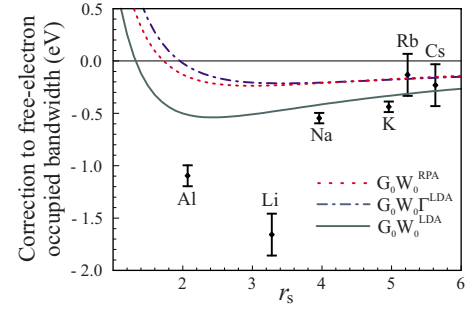


FIG. 5. (Color online) Correction to the free-electron occupied bandwidth—comparison with experiments. $G_0W_0^{\text{LDA}}$ has the most significant narrowing of the band in the relevant density region. $G_0W_0\Gamma^{\text{LDA}}$ is not very different from $G_0W_0^{\text{RPA}}$. Note that a jellium calculation does not include the contribution from the crystal lattice potential.

the chemical potential from the LDA surface calculation, μ^{LDA} . Since the exact self-energy for jellium must fulfill the condition

$$\text{Re}[\Sigma_{\mathbf{k}_F}(\varepsilon_F)] = V_{\text{xc}}, \quad (17)$$

we see that the LDA (taken from highly accurate QMC calculations) corresponds to the exact result if one assumes that the bulk is accurately modeled by jellium. Comparing with Table V and Fig. 6, we see that $G_0W_0^{\text{RPA}}$ is closest to the exact result and $G_0W_0^{\text{LDA}}$ is slightly further away, while $G_0W_0\Gamma^{\text{LDA}}$ is even worse.

This leads us to conclude that $G_0W_0\Gamma^{\text{LDA}}$ is unphysical in the sense that a vertex correction derived from a self-energy approximation with a completely local dependence on the density (like the LDA) will have pathological features. This is most probably due to the improper behavior of the spectral function of the screened interaction, as is demonstrated in the final section of this paper.

VII. DISCUSSION AND CONCLUSIONS

We have presented $G_0W_0^{\text{LDA}}$ and $G_0W_0\Gamma^{\text{LDA}}$ calculations for isolated atoms and jellium. We see that $G_0W_0\Gamma^{\text{LDA}}$ worsens results in all cases compared to the common $G_0W_0^{\text{RPA}}$ approximation.

A proper *ab initio* vertex correction for calculations on an arbitrary system should be derived from the starting approximation for the self-energy. In this work, we have shown that in practice, vertex corrections derived from a local-density approximation to the self-energy (like the LDA) are pathological when applied to both the self-energy and the screened interaction. The work function of aluminum was used to confirm that the value of the chemical potential in $G_0W_0\Gamma^{\text{LDA}}$ is far from the correct result.

An indication of why a local correction in both W and Σ performs so poorly has been discussed previously by Hindgren and Almladh⁵⁸ and investigated in excitonic effects on wide-band-gap semiconductors by Marini and co-workers.^{59,60} Both types of vertex corrections lead to a modified screened interaction $\tilde{W} = \tilde{\varepsilon}^{-1}v$. The spectral function

TABLE V. The work function of aluminum ($r_s=2.07$)—compared to experiment. The last four columns show the deviation from the experimental value. The LDA surface calculation corresponds to the exact result if jellium is used to model the bulk Fermi energy. $G_0W_0^{\text{RPA}}$ and $G_0W_0^{\text{LDA}}$ are closer, while $G_0W_0\Gamma^{\text{LDA}}$ is much worse.

Φ Al	Expt. (eV) ^a	LDA ^b	$G_0W_0^{\text{RPA}}$	$G_0W_0\Gamma^{\text{LDA}}$	$G_0W_0^{\text{LDA}}$
(100)	4.41	-0.14	0.28	-1.19	0.45
(110)	4.06	-0.18	0.24	-1.23	0.41
(111)	4.24	-0.06	0.36	-1.11	0.53

^aSee Ref. 56.

^bSee Ref. 57.

of this, which is required to be positive semidefinite for $\omega \leq 0$ and negative semidefinite otherwise, is given by

$$B_{\mathbf{q}}(\omega) = -\frac{\text{sgn}(\omega)}{\pi} \text{Im}[\tilde{W}_{\mathbf{q}}(\omega)] = \frac{\text{sgn}(\omega)}{\pi} \frac{\text{Im}[\tilde{\epsilon}_{\mathbf{q}}(\omega)]}{|\tilde{\epsilon}_{\mathbf{q}}(\omega)|^2} v_{\mathbf{q}}, \quad (18)$$

so it inherits whatever properties of definiteness the imaginary part of the dielectric function has. Now, for $G_0W_0\Gamma^{\text{LDA}}$, this is given by

$$\text{Im}[\tilde{\epsilon}_{\mathbf{q}}(\omega)] = -(v_{\mathbf{q}} + K_{\text{xc}}) \text{Im}[\chi_{\mathbf{q}}^0(\omega)]. \quad (19)$$

Since the RPA response function χ_0 will have the correct analytical properties by construction, this expression will obviously change sign whenever K_{xc} —which is strictly negative for all densities and a negative constant for jellium—is larger in magnitude than $v_{\mathbf{q}}$, which decays as $1/q^2$. This will thus lead to a spectral function with the wrong sign, which is entirely unphysical. For jellium, isolated atoms, or any sparse enough condensed state, this is guaranteed to happen

because $K_{\text{xc}} \rightarrow -\infty$ for low densities. Inspection of the dielectric function in $G_0W_0^{\text{LDA}}$,

$$\text{Im}[\tilde{\epsilon}_{\mathbf{q}}(\omega)] = -\frac{v_{\mathbf{q}} \text{Im}[\chi_{\mathbf{q}}^0(\omega)]}{|1 - K_{\text{xc}}\chi_{\mathbf{q}}^0(\omega)|^2}, \quad (20)$$

illustrates that it cannot suffer from the same pathology. Since Eq. (20) ensures that the static structure factor has the correct behavior for both $G_0W_0^{\text{LDA}}$ and $G_0W_0\Gamma^{\text{LDA}}$, no conclusions can be drawn on the reason for the overly positive value of the pair-correlation function of jellium when $r \rightarrow 0$, except that it must depend on the high k behavior of the denominator. We note that none of the calculations have been carried out self-consistently; it is possible that the vertices presented here go some way to improve self-consistent GW results.⁶⁴

One possibility of the failure of the LDA starting point with the inclusion of the theoretically consistent vertex is the self-interaction error the LDA orbitals carry with them. Any starting point with an inherent self-interaction error should lead to correcting terms in the diagrammatic expansion. It is possible that the first-order correction, such as $G_0W_0\Gamma^{\text{LDA}}$, is not enough and higher order corrections must be applied. A vertex derived from a second iteration of Hedin's equations does indeed lead to further and more complicated diagrams than the equivalent vertex from a Hartree starting point. Unfortunately, these diagrams are of prohibitive complexity for practical calculations.

It is still not understood why a correction in W only (in a TDDFT-like manner) seems to work as well as it does. There is a similarity here with the way that the Bethe-Salpeter equation (BSE) is usually applied for the calculation of optical spectra. There too, it is well known that, in theory, inclusion of a screened interaction in electron-hole excitations should be accompanied by an inclusion of the double-exchange term in $\tilde{\Sigma}$ but this has been proven to worsen results. Recently, Tiago and Chelikowsky⁶² have used a $G_0W_0^{\text{LDA}}$ vertex in conjunction with an efficient numerical implementation of the BSE for isolated molecules and have shown that the inclusion of a TD-LDA vertex gives very good results over a wide range of structural configurations in excited states.

For atomic helium and beryllium, $G_0W_0^{\text{LDA}}$ is very similar

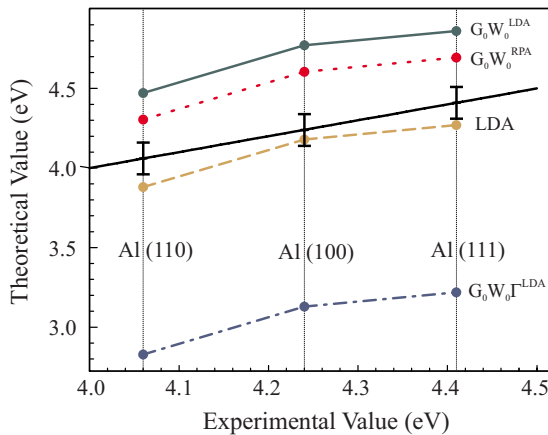


FIG. 6. (Color online) The work function of aluminum ($r_s=2.07$)—compared to experiment. The LDA surface calculation corresponds to the exact result if jellium is used to model the bulk Fermi energy. $G_0W_0^{\text{RPA}}$ and $G_0W_0^{\text{LDA}}$ are closer, while $G_0W_0\Gamma^{\text{LDA}}$ is much worse. The colored lines are there to guide the eyes. The black line corresponds to the perfect agreement with experiment (error bars indicate experimental uncertainty).

to the $G_0W_0^{\text{RPA}}$ result but slightly worse in neon, while in jellium, the bandwidth is improved. Hence, $G_0W_0^{\text{LDA}}$ may be a local and easily implementable way to improve quasiparticle results in extended systems.

Overall, vertices based on the local density clearly have their limitations, arriving in part from the wave vector independent character of K_{xc} . It should be fruitful to explore vertices that incorporate nonlocal-density dependence and reflect the nonlocal character of the original self-energy operator.

ACKNOWLEDGMENTS

The authors would like to thank Ulf von Barth, Carl-Olof Almbladh, Peter Bokes, Arno Schindlmayr, Matthieu Verstraete, Steven Tear, and John Trail for helpful discussions. This research was supported in part by the European Union (Contract No. NMP4-CT-2004-500198, “Nanoquanta” Network of Excellence), the Spanish MEC (Project No. FIS2004-05035-C03-03), and the Ramón y Cajal Program (PGG).

*Present address: Theory of Condensed Matter Group, Cavendish Laboratory, University of Cambridge, J. J. Thomson Avenue, Cambridge CB3 0HE, United Kingdom; ajm255@cam.ac.uk

†Present address: Materials Research Laboratory, University of California, Santa Barbara, CA 93106-5121.

¹W. G. Aulbur, L. Jönsson, and J. W. Wilkins, *Solid State Phys.* **54**, 1 (2000).

²F. Aryasetiawan and O. Gunnarsson, *Rep. Prog. Phys.* **61**, 237 (1998).

³L. Hedin and S. Lundqvist, *Solid State Phys.* **23**, 2 (1969).

⁴L. Hedin, *Phys. Rev.* **139**, A796 (1965).

⁵R. W. Godby, M. Schlüter, and L. J. Sham, *Phys. Rev. Lett.* **56**, 2415 (1986).

⁶P. Rinke, A. Qteish, J. Neugebauer, C. Freysoldt, and M. Scheffler, *New J. Phys.* **7**, 126 (2005).

⁷W. Nelson, P. Bokes, P. Rinke, and R. W. Godby, *Phys. Rev. A* **75**, 032505 (2007).

⁸R. Del Sole, L. Reining, and R. W. Godby, *Phys. Rev. B* **49**, 8024 (1994).

⁹We have modified the notation of Del Sole *et al.* to clarify the precise nature of the different approximate vertices: we use $G_0W_0\Gamma^{\text{LDA}}$ in place of GWT and $G_0W_0^{\text{LDA}}$ in place of GWK_{xc} .

¹⁰M. S. Hybertsen and S. G. Louie, *Phys. Rev. B* **34**, 5390 (1986).

¹¹A. Schindlmayr and R. W. Godby, *Phys. Rev. Lett.* **80**, 1702 (1998).

¹²F. Bechstedt, K. Tenelsen, B. Adolph, and R. Del Sole, *Phys. Rev. Lett.* **78**, 1528 (1997).

¹³J. E. Northrup, M. S. Hybertsen, and S. G. Louie, *Phys. Rev. Lett.* **59**, 819 (1987).

¹⁴M. P. Surh, J. E. Northrup, and S. G. Louie, *Phys. Rev. B* **38**, 5976 (1988).

¹⁵E. Jensen and E. W. Plummer, *Phys. Rev. Lett.* **55**, 1912 (1985).

¹⁶Kenneth W.-K. Shung, B. E. Sernelius, and G. D. Mahan, *Phys. Rev. B* **36**, 4499 (1987).

¹⁷X. Zhu and A. W. Overhauser, *Phys. Rev. B* **33**, 925 (1986).

¹⁸H. O. Frota and G. D. Mahan, *Phys. Rev. B* **45**, 6243 (1992).

¹⁹H. Yasuhara and Y. Takada, *Phys. Rev. B* **43**, 7200 (1991).

²⁰B. S. Itchkawitz, I.-W. Lyo, and E. W. Plummer, *Phys. Rev. B* **41**, 8075 (1990).

²¹I.-W. Lyo and E. W. Plummer, *Phys. Rev. Lett.* **60**, 1558 (1988).

²²Y. Takada, *Phys. Rev. Lett.* **87**, 226402 (2001).

²³W. Ku, A. G. Eguluz, and E. W. Plummer, *Phys. Rev. Lett.* **85**, 2410 (2000).

²⁴H. Yasuhara, S. Yoshinaga, and M. Higuchi, *Phys. Rev. Lett.* **85**, 2411 (2000).

²⁵H. Yasuhara, S. Yoshinaga, and M. Higuchi, *Phys. Rev. Lett.* **83**, 3250 (1999).

²⁶E. L. Shirley and R. M. Martin, *Phys. Rev. B* **47**, 15404 (1993).

²⁷J. M. Luttinger and J. C. Ward, *Phys. Rev.* **118**, 1417 (1960).

²⁸N. E. Dahlen, R. van Leeuwen, and U. von Barth, *Phys. Rev. A* **73**, 012511 (2006).

²⁹N. E. Dahlen and U. von Barth, *Phys. Rev. B* **69**, 195102 (2004).

³⁰A. Stan, N. E. Dahlen, and R. van Leeuwen, *Europhys. Lett.* **76**, 2988 (2006).

³¹S. Verdonck, D. Van Neck, P. W. Ayers, and M. Waroquier, *Phys. Rev. A* **74**, 062503 (2006).

³²G. Baym and L. P. Kadanoff, *Phys. Rev.* **124**, 287 (1961).

³³H. N. Rojas, R. W. Godby, and R. J. Needs, *Phys. Rev. Lett.* **74**, 1827 (1995).

³⁴P. Rinke, K. Delaney, P. García-González, and R. W. Godby, *Phys. Rev. A* **70**, 063201 (2004).

³⁵K. Delaney, P. García-González, A. Rubio, P. Rinke, and R. W. Godby, *Phys. Rev. Lett.* **93**, 249701 (2004).

³⁶B. Holm and F. Aryasetiawan, *Phys. Rev. B* **62**, 4858 (2000).

³⁷A. Ma, N. D. Drummond, M. D. Towler, and R. J. Needs, *Phys. Rev. E* **71**, 066704 (2005).

³⁸C. C. J. Roothaan, L. M. Sachs, and A. W. Weiss, *Rev. Mod. Phys.* **32**, 186 (1960).

³⁹C.-J. Huang, C. J. Umrigar, and M. P. Nightingale, *J. Chem. Phys.* **107**, 3007 (1997).

⁴⁰R. J. Gdanitz, *J. Chem. Phys.* **109**, 9795 (1998).

⁴¹P. García-González and R. W. Godby, *Phys. Rev. B* **63**, 075112 (2001).

⁴²J. P. Perdew and A. Zunger, *Phys. Rev. B* **23**, 5048 (1981).

⁴³J. B. Krieger, Y. Li, and G. J. Iafrate, *Phys. Rev. A* **45**, 101 (1992).

⁴⁴B. Holm and U. von Barth, *Phys. Rev. B* **57**, 2108 (1998).

⁴⁵K. S. E. Eikema, W. Ubachs, W. Vassen, and W. Hogervorst, *Phys. Rev. A* **55**, 1866 (1997).

⁴⁶S. D. Bergeson, A. Balakrishnan, K. G. H. Baldwin, T. B. Lucatorto, J. P. Marangos, T. J. McIlrath, T. R. O’Brien, S. L. Rolston, C. J. Sansonetti, J. Wen, N. Westbrook, C. H. Cheng, and E. E. Eyler, *Phys. Rev. Lett.* **80**, 3475 (1998).

⁴⁷A. E. Kramida and W. C. Martin, *J. Phys. Chem. Ref. Data* **26**, 1185 (1997).

⁴⁸V. Kaufman and L. Minnhagen, *J. Opt. Soc. Am.* **62**, 92 (1972).

⁴⁹A. Fleszar and W. Hanke, *Phys. Rev. B* **56**, 10228 (1997).

⁵⁰C.-O. Almbladh and A. Schindlmayr (private communication).

⁵¹P. Gori-Giorgi, F. Sacchetti, and G. B. Bachelet, *Phys. Rev. B* **61**, 7353 (2000).

⁵²G. D. Mahan and B. E. Sernelius, *Phys. Rev. Lett.* **62**, 2718 (1989).

⁵³H. J. Levinson, F. Greuter, and E. W. Plummer, *Phys. Rev. B* **27**, 727 (1983).

⁵⁴R. S. Crisp and S. E. Williams, *Philos. Mag.* **8**, 1205 (1960).

⁵⁵N. V. Smith and G. B. Fisher, *Phys. Rev. B* **3**, 3662 (1971).

⁵⁶H. B. Michaelson, *J. Appl. Phys.* **48**, 4729 (1977).

⁵⁷P. A. Serena, J. M. Soler, and N. García, *Phys. Rev. B* **37**, 8701 (1988).

⁵⁸M. Hindgren and C.-O. Almbladh, *Phys. Rev. B* **56**, 12832 (1997).

⁵⁹Andrea Marini and Angel Rubio, *Phys. Rev. B* **70**, 081103(R) (2004).

⁶⁰A. Marini, R. Del Sole, and A. Rubio, *Time-Dependent Density Functional Theory*, Lecture Notes in Physics Vol. 706, edited by M. A. L. Marques, C. A. Ulrich, F. Nogueira, A. Rubio, K. Burke, and E. K. U. Gross, (Springer, New York, 2006), Chap. 10, pp. 173–178.

⁶¹A. Fleszar and W. Hanke, *Phys. Rev. B* **71**, 045207 (2005).

⁶²M. L. Tiago and J. R. Chelikowsky, *Phys. Rev. B* **73**, 205334 (2006).

⁶³We compute quantities for the nonrelativistic, all-electron Hamiltonian.

⁶⁴Recently, Fleszar and Hanke (Ref. 61) have also used the $G_0W_0\Gamma^{\text{LDA}}$ vertex and noted improvement in band gaps and the energy positions relative to the valence band minimum for the computationally difficult II^{B} -VI semiconductors when the $G_0W_0\Gamma^{\text{LDA}}$ method is used in conjunction with G and W partially updated through one previous iteration of Hedin's equations.